

## Carbon-sulfur bond formation by reductive elimination of gold(III) thiolates†

Lucy Currie, Luca Rocchigiani, David L. Hughes and Manfred Bochmann\*

### SUPPORTING INFORMATION

1. Kinetic measurements
2. NMR spectra

#### Kinetic investigations

**1a/b** (0.005 g, 0.0087 mmol) was dissolved in dry  $\text{CD}_2\text{Cl}_2$  (0.6 mL) in a J-Young NMR tube and an initial  $^1\text{H}$  NMR spectra was recorded to lock and shim the sample. In the open air, adamantyl thiol (at varying concentrations) was added to the NMR tube and the reaction was followed *in situ* by  $^1\text{H}$  NMR spectroscopy. Different intervals between the spectra were used according to the thiol concentration.

Absolute concentration values were evaluated by relative integration to an external standard. The spectra were processed and the normalized concentration of **1a/b** was monitored over the course of the reaction by comparing the intensity of t-butyl signal with the spectrum at  $t = 0$ .

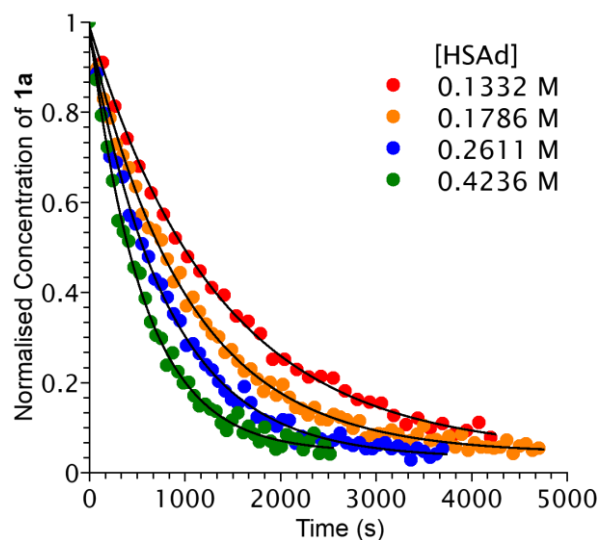


Figure 1, The decay of **1a** at different concentrations of HSAd

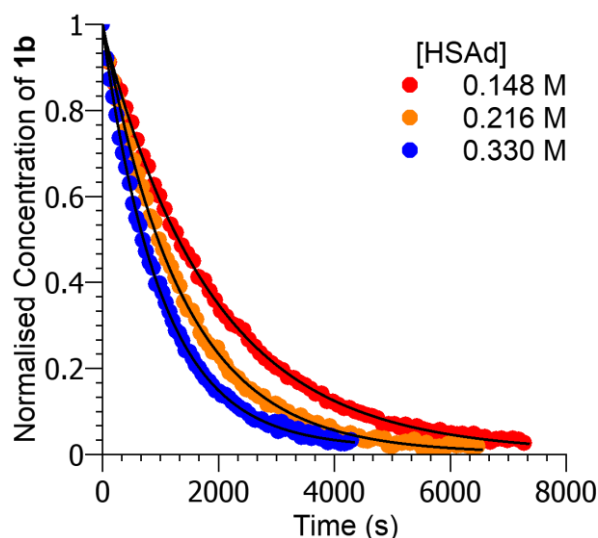


Figure 2, The decay of **1b** at different concentrations of HSAd

### Diffusion NMR

Diffusion NMR was used to investigate the hydrodynamic dimensions of the species obtained after C–S reductive elimination of (C<sup>N</sup>C)AuCl in the presence of adamantyl thiol. As described before, at the end of the reaction, the mixture is composed by free adamantyl thiol, **3a** and an additional adamantyl species, reasonably assigned to the Au(I) complex formed upon elimination of the ligand.

<sup>1</sup>H PGSE NMR experiments were performed by using a double stimulated echo sequence with longitudinal eddy delay on a Bruker DRX 300 spectrometer equipped with a smartprobe and Z-gradient coil, at 297K without spinning. The decay of the signals (*I*) as a function of the applied gradient (*G*, Figure 3) was treated as reported in the literature<sup>1</sup> to obtain hydrodynamic data values, under the spherical approximation. The CD<sub>2</sub>Cl<sub>2</sub> solvent was used as internal standard.

The interpolation of the experiment reported in Figure 3, gave hydrodynamic volume values of 184 and 727 Å<sup>3</sup> for adamantyl thiol and **3a**, respectively. The Au(I) complex showed a hydrodynamic volume of 1500 Å<sup>3</sup>, which is about 8 times larger than free thiol. Therefore, it can be reasonably assumed that the Au(I) product exists as a small [ClAuSAd]<sub>*n*</sub>H<sub>*n*</sub> cluster, with an average *n* close to 7.

1) A. Macchioni, G. Ciancaleoni, C. Zuccaccia, D. Zuccaccia, *Chem. Soc. Rev.* **2008**, 37, 479.

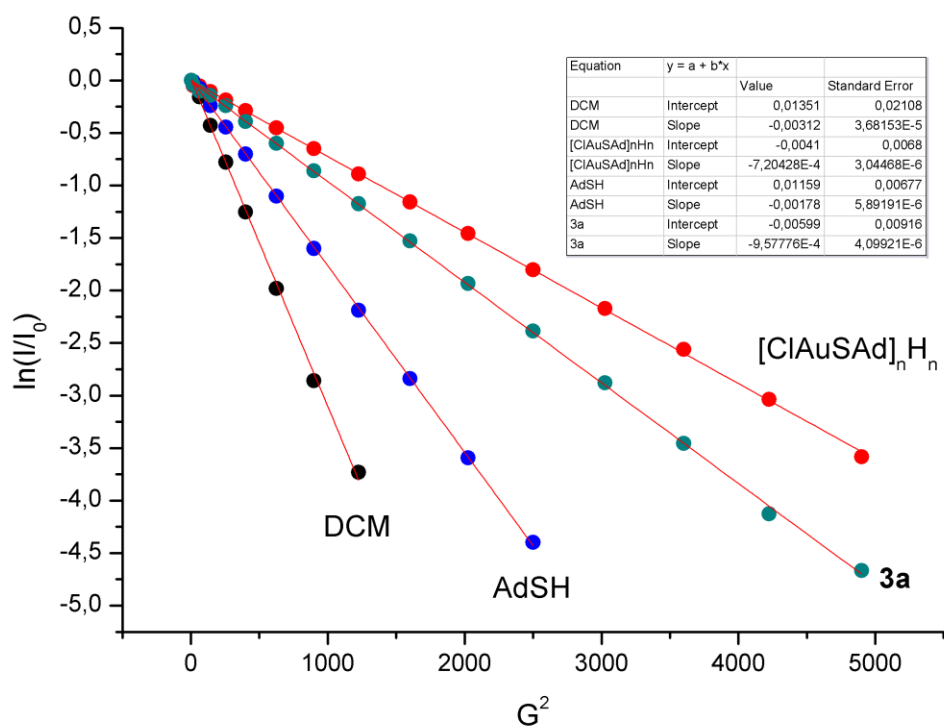


Figure 3. trends of  $\ln(I/I_0)$  versus  $G^2$  for the components of the mixture obtained after the reaction of **1a** with AdSH.

# NMR spectra

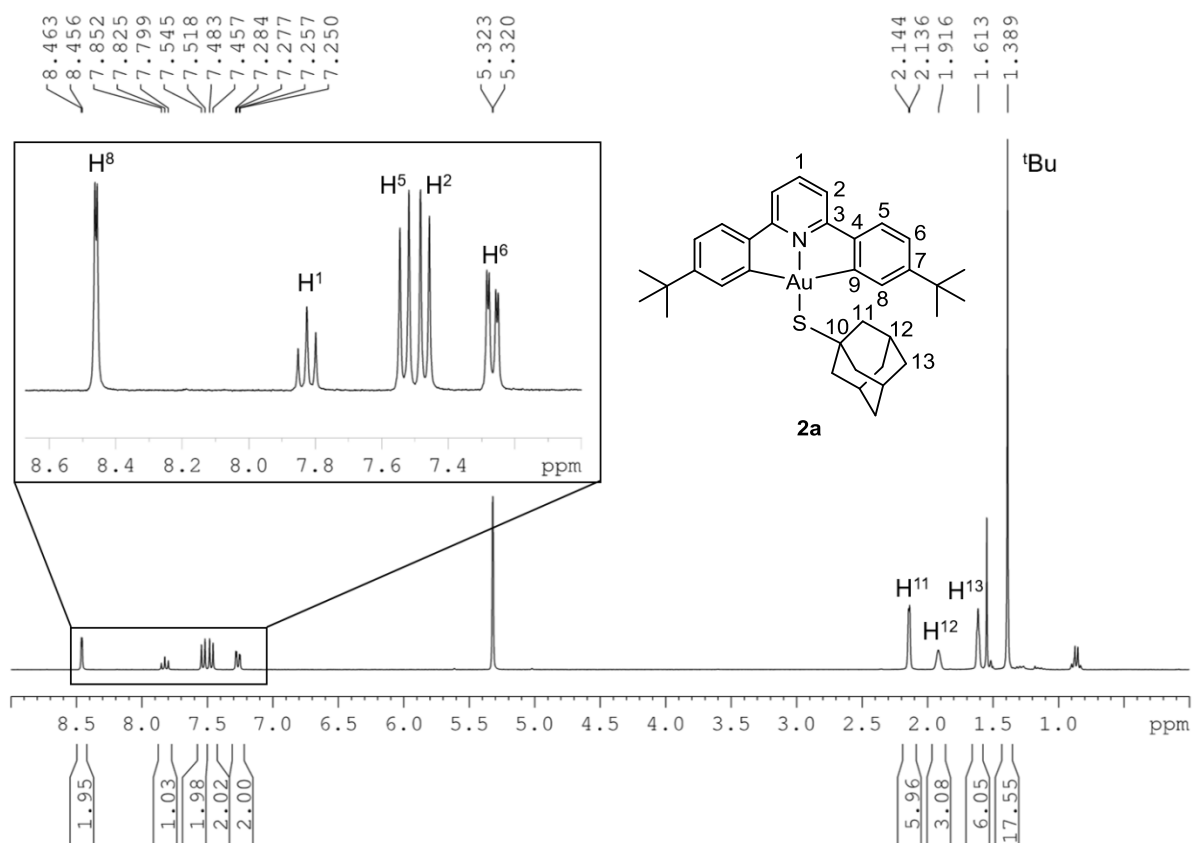


Figure 4, <sup>1</sup>H NMR spectrum of **2a** (CD<sub>2</sub>Cl<sub>2</sub>, 25 °C).

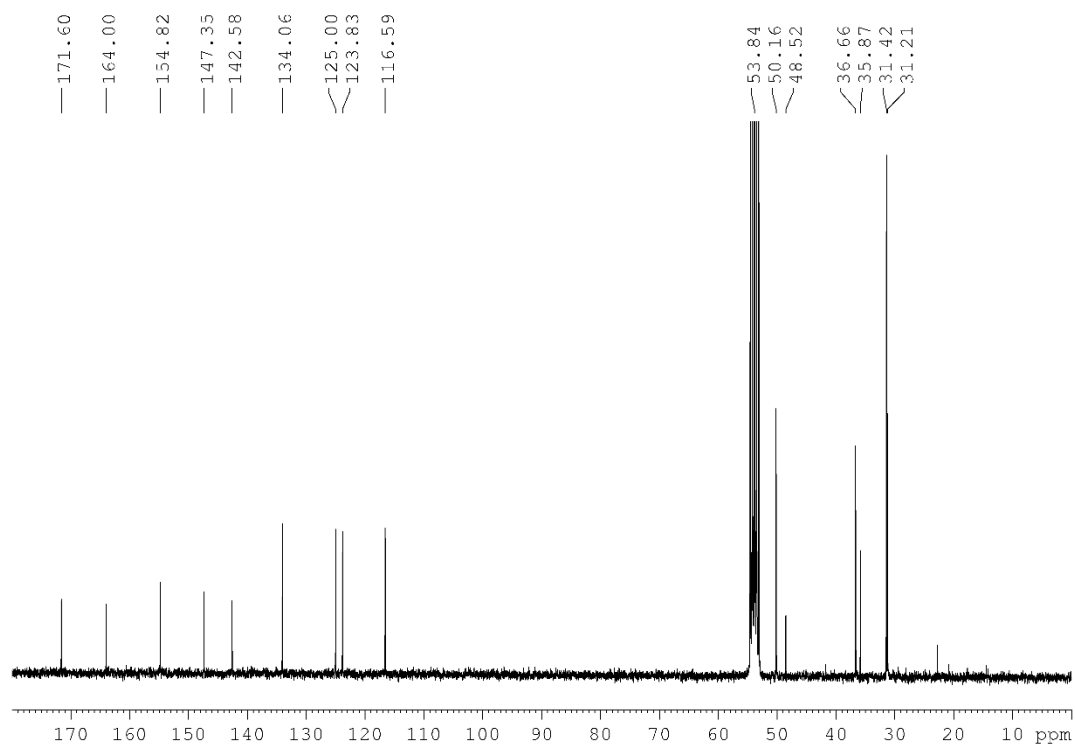


Figure 5, <sup>13</sup>C NMR spectrum of **2a** (CD<sub>2</sub>Cl<sub>2</sub>, 25 °C).

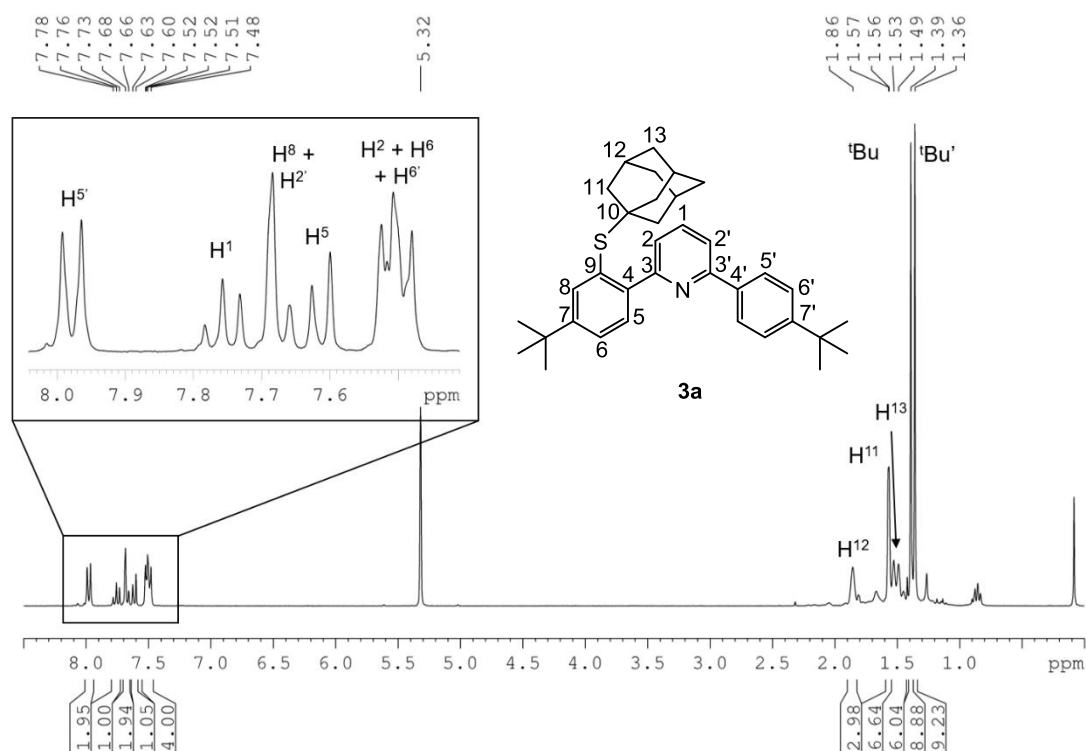


Figure 6, <sup>1</sup>H NMR spectrum of **3a** (CD<sub>2</sub>Cl<sub>2</sub>, 25 °C).

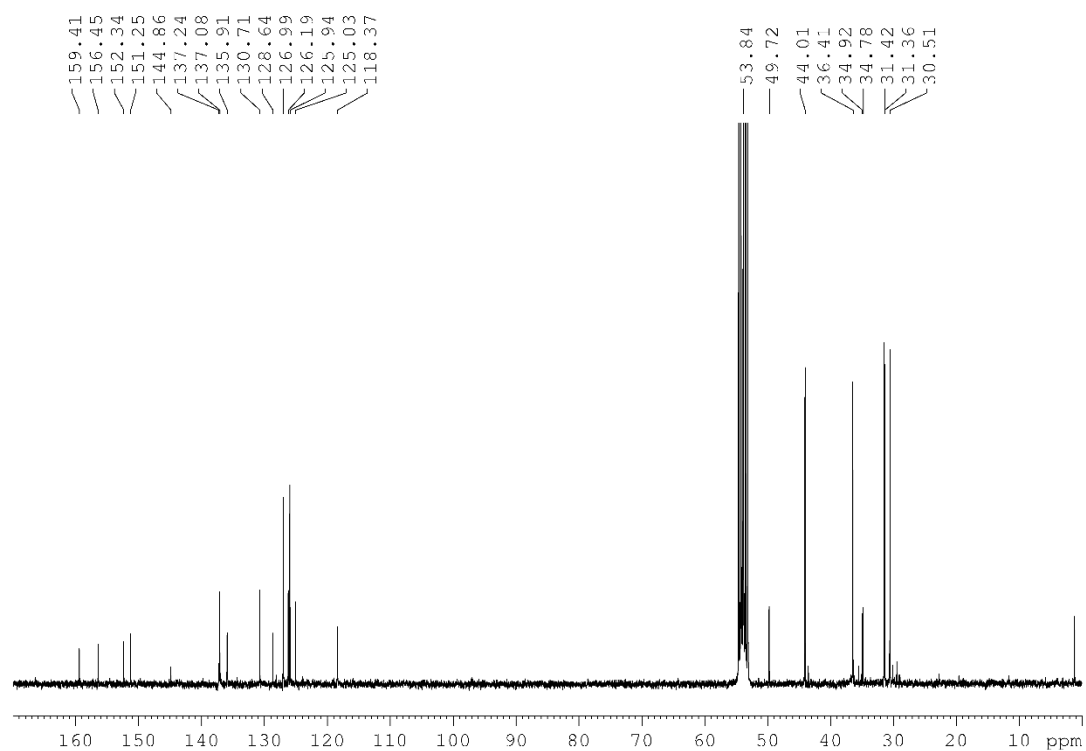


Figure 7, <sup>13</sup>C NMR spectrum of **3a** (CD<sub>2</sub>Cl<sub>2</sub>, 25 °C).

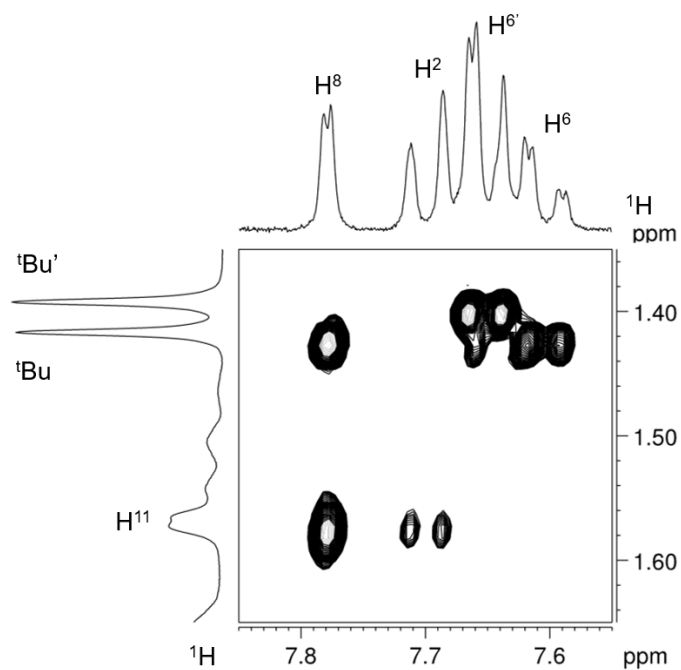


Figure 8,  $^1\text{H}$  NOESY NMR spectrum of **3a** showing through space interactions of  $\text{H}^{11}$  with both  $\text{H}^8$  and  $\text{H}^2$  ( $\text{CD}_2\text{Cl}_2$ , 25  $^\circ\text{C}$ ).

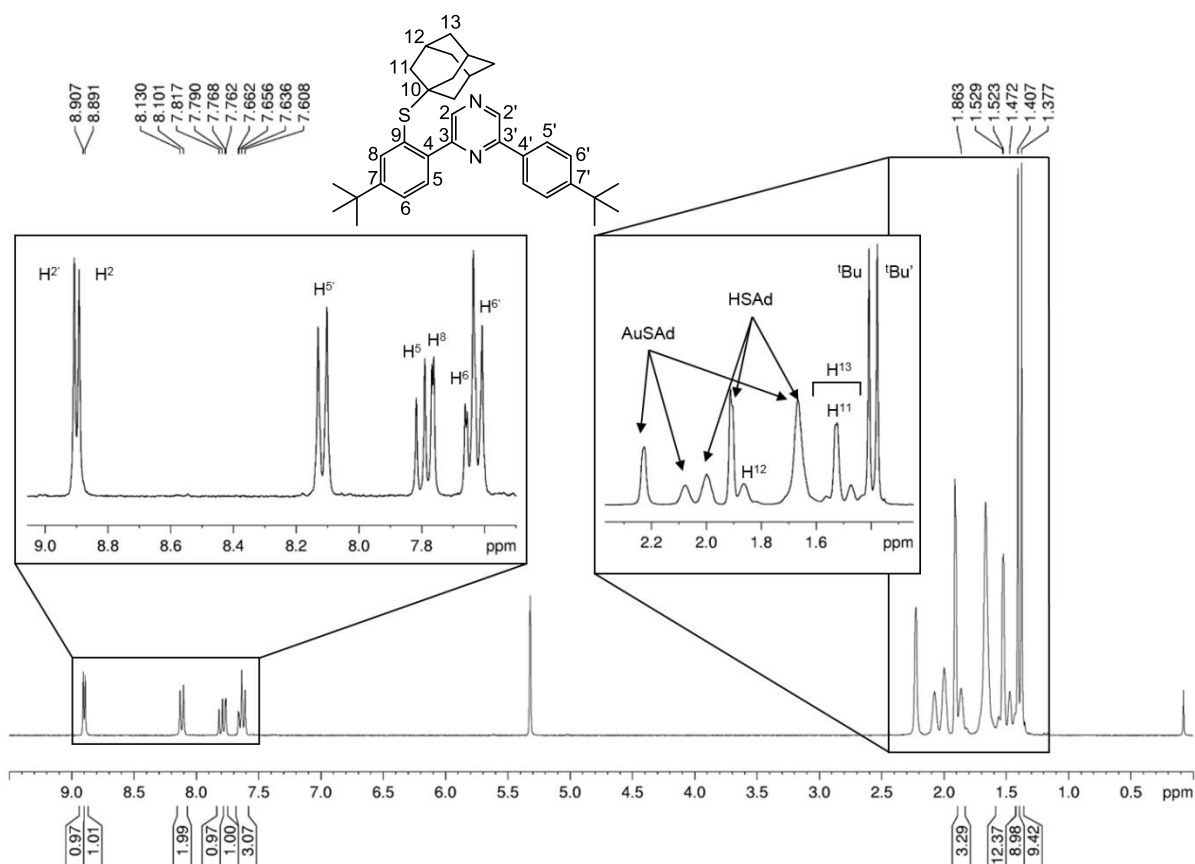


Figure 9,  $^1\text{H}$  NMR spectrum of the *in situ* synthesis of **3b** ( $\text{CD}_2\text{Cl}_2$ , 25  $^\circ\text{C}$ ).

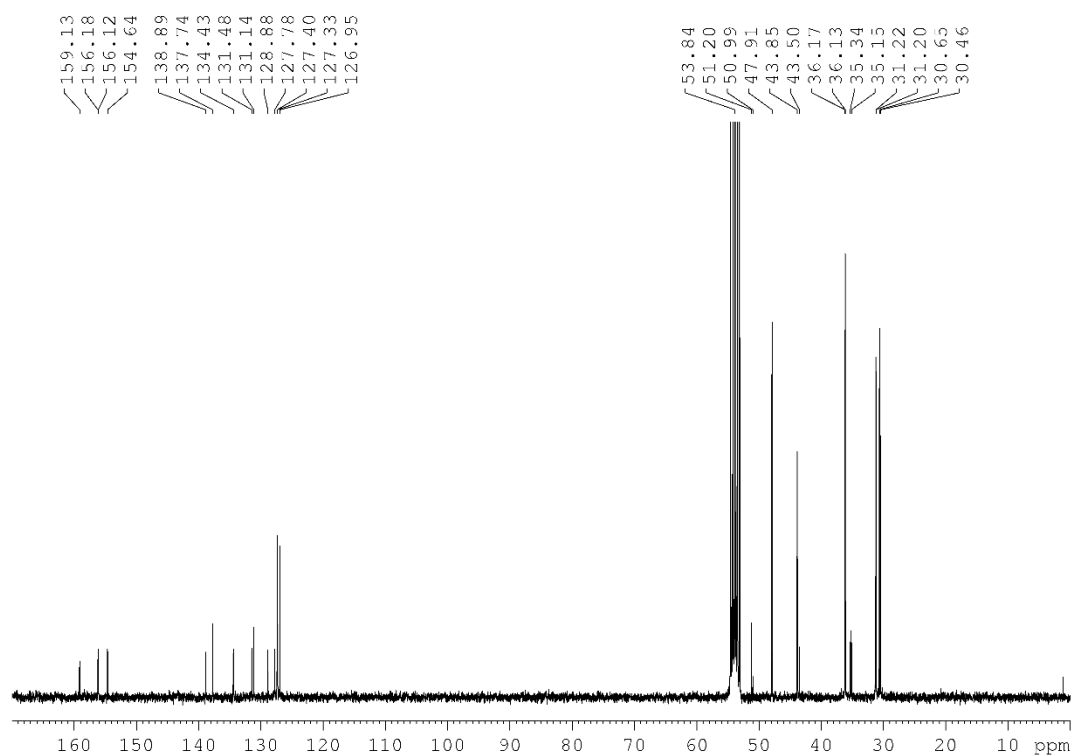


Figure 10,  $^{13}\text{C}$  NMR spectrum of the *in situ* synthesis of **3b** ( $\text{CD}_2\text{Cl}_2$ , 25 °C).

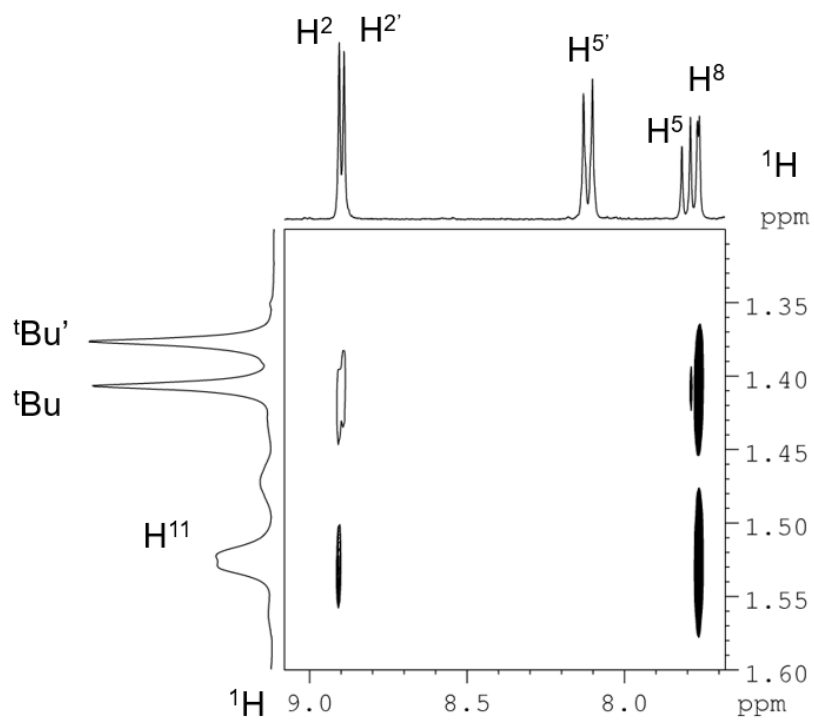


Figure 11,  $^1\text{H}$  NOESY NMR spectrum of **3b** showing through space interactions between  $\text{H}^{11}$  and  $\text{H}^2$  and  $\text{H}^8$  ( $\text{CD}_2\text{Cl}_2$ , 25 °C).

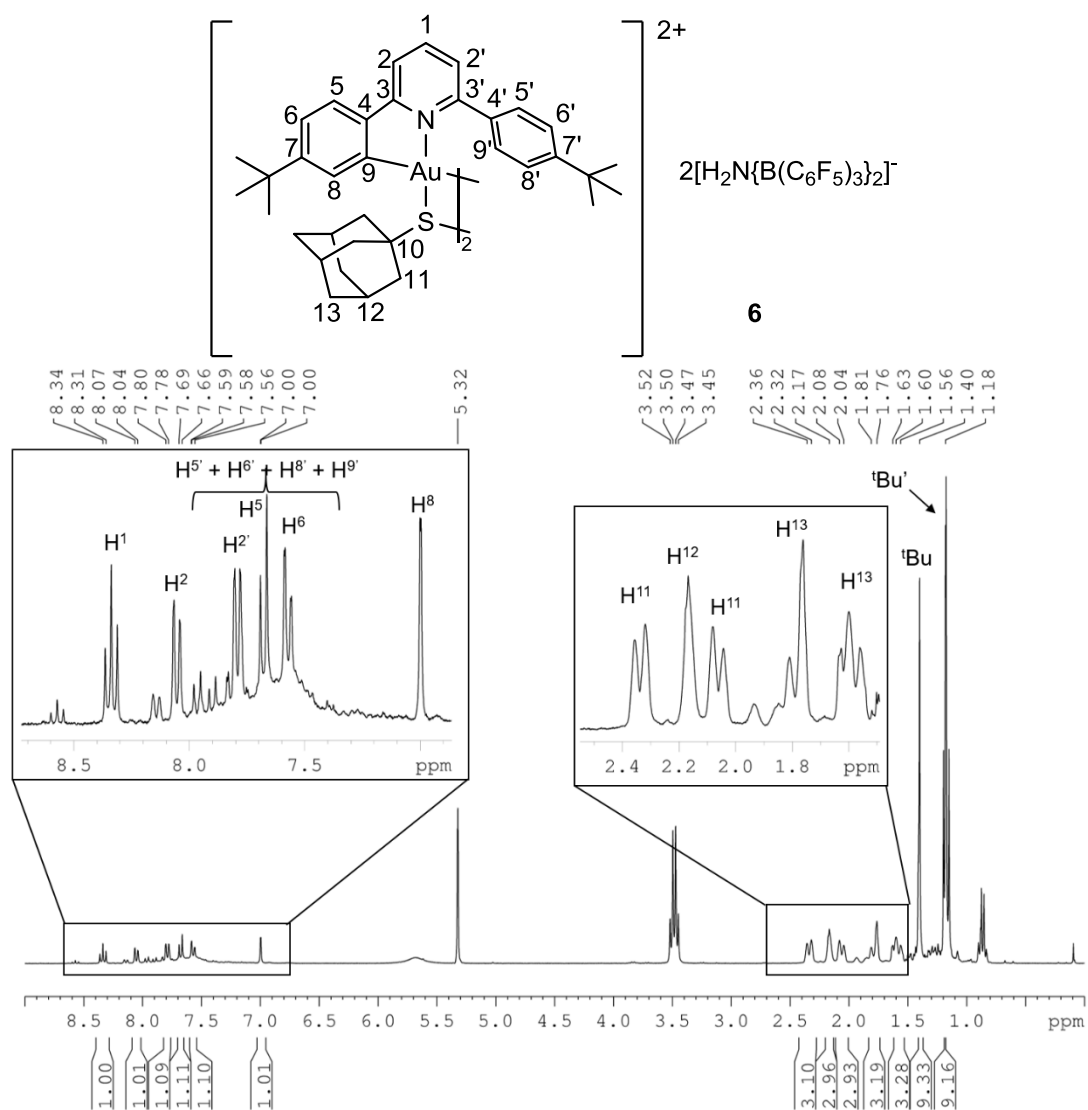


Figure 12,  $^1\text{H}$  NMR spectrum of **6** (CD $_2$ Cl $_2$ , 25 °C).



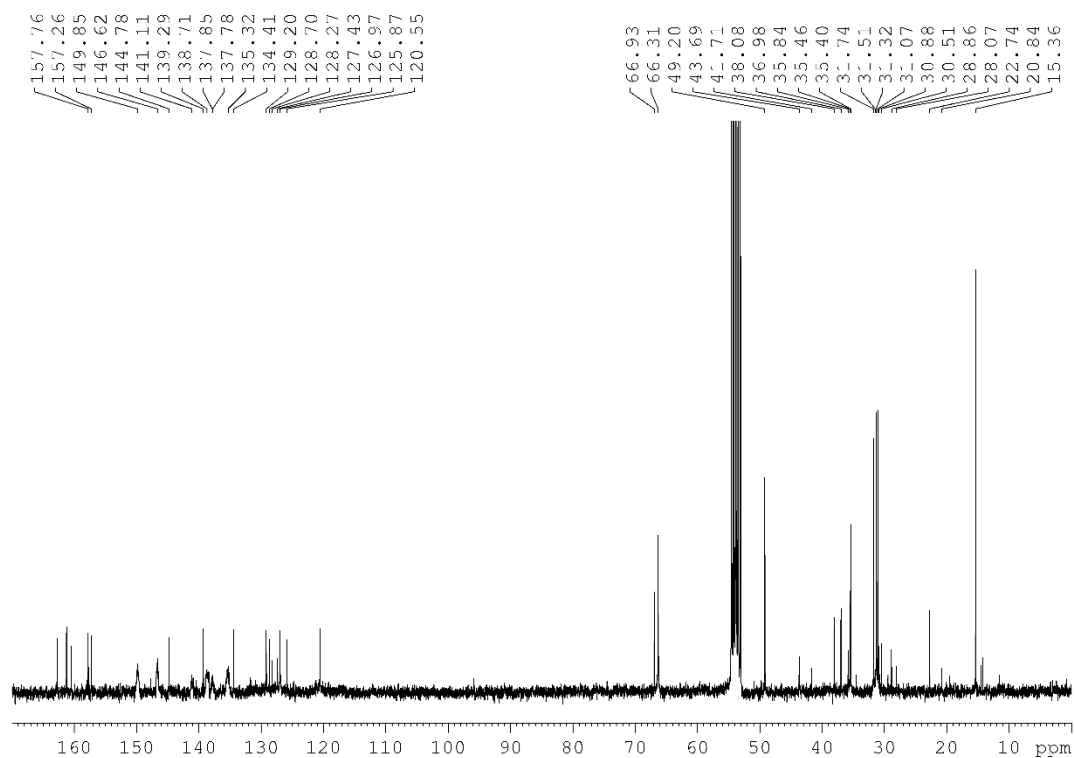


Figure 13,  $^{13}\text{C}$  NMR spectrum of **6** ( $\text{CD}_2\text{Cl}_2$ , 25  $^\circ\text{C}$ ).

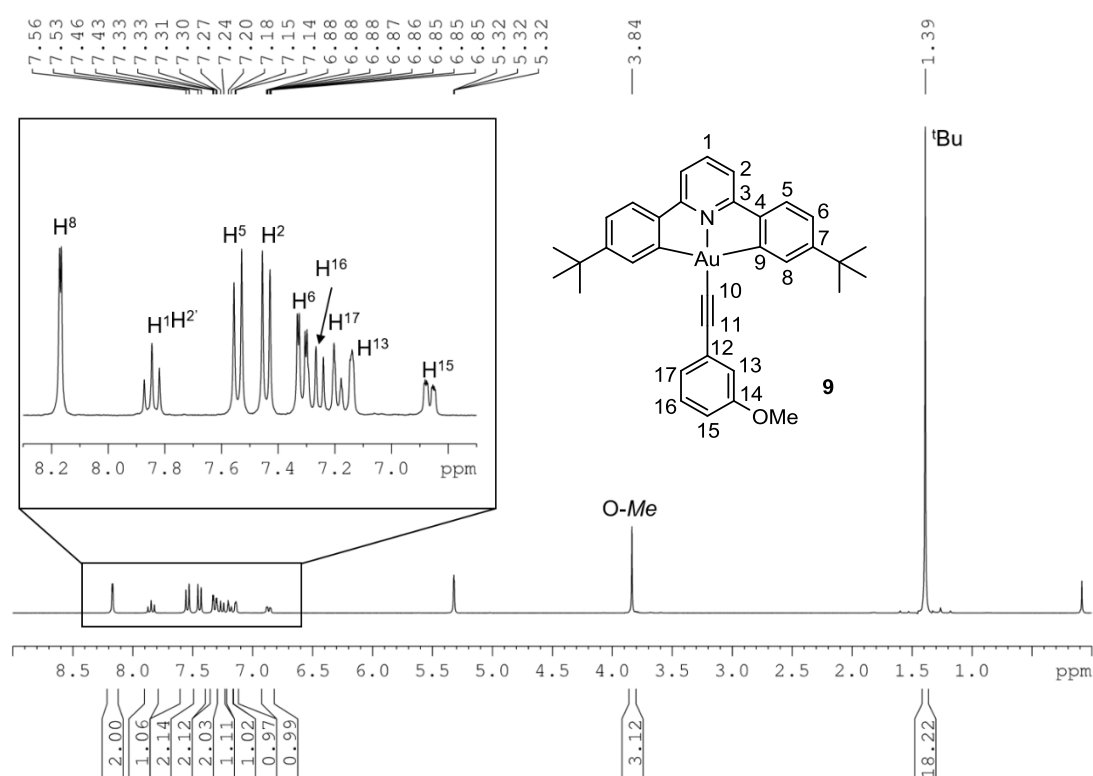


Figure 14,  $^1\text{H}$  NMR spectrum of **9** ( $\text{CD}_2\text{Cl}_2$ , 25  $^\circ\text{C}$ ).

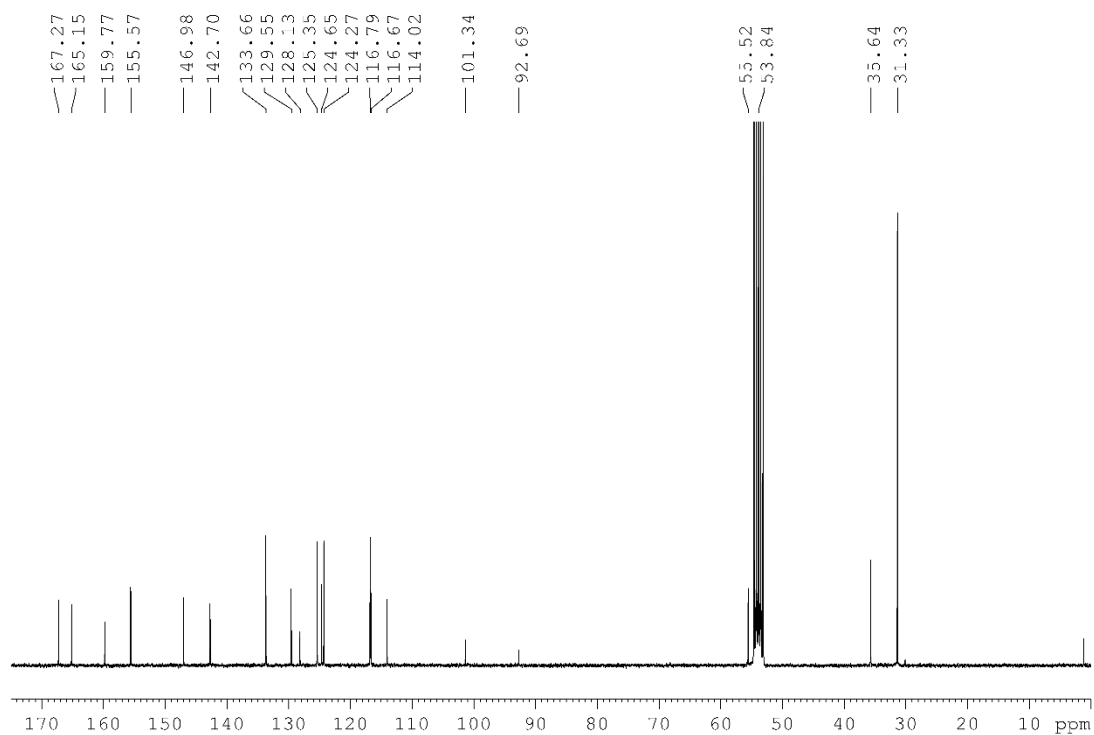


Figure 15,  $^{13}\text{C}$  NMR spectrum of **9** ( $\text{CD}_2\text{Cl}_2$ , 25 °C).

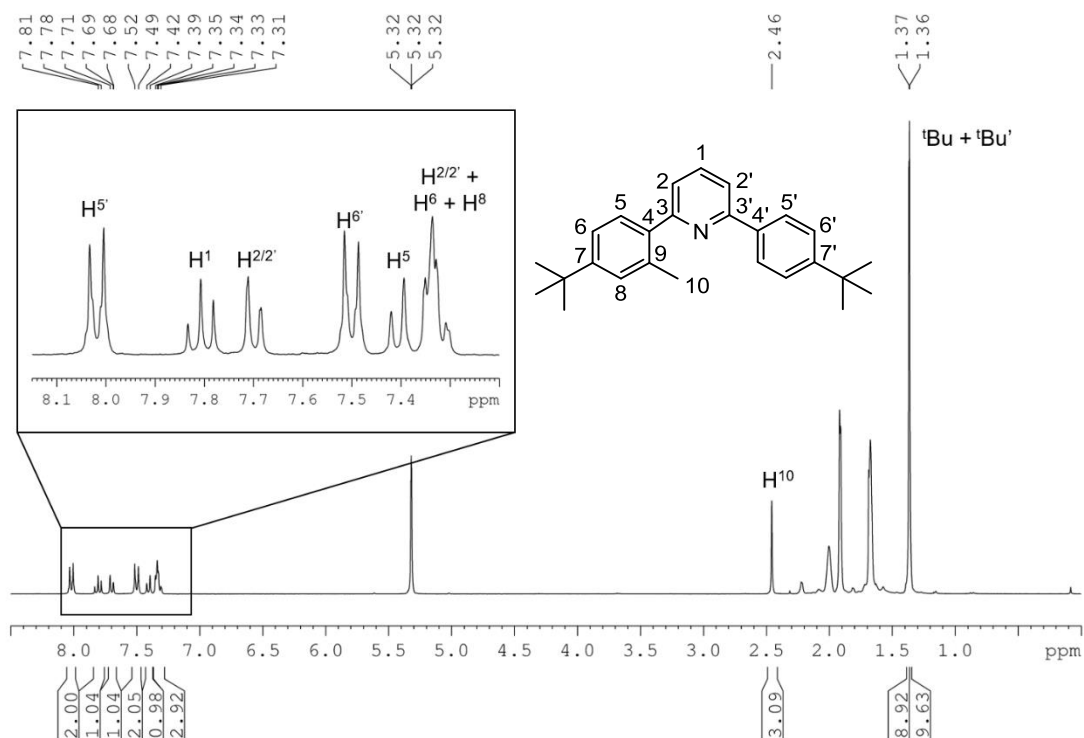


Figure 18,  $^1\text{H}$  NMR spectrum of C-Me coupling product **10** ( $\text{CD}_2\text{Cl}_2$ , 25 °C).

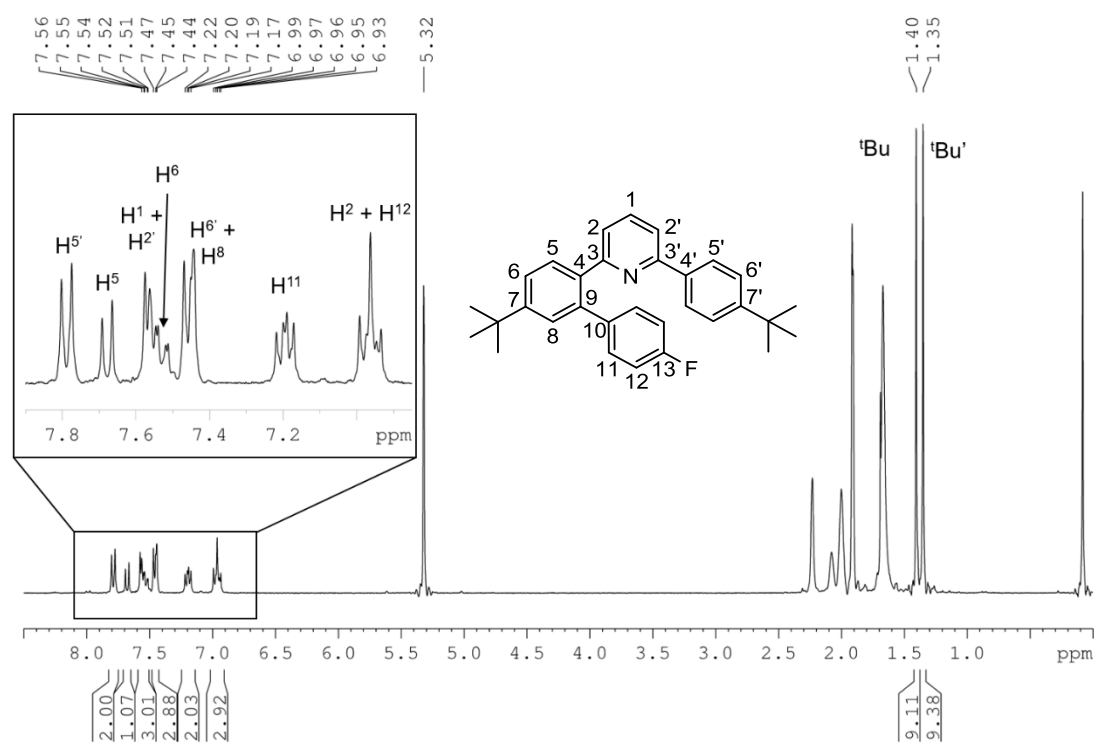


Figure 16,  $^1\text{H}$  NMR spectrum of the C-C $_6\text{H}_4\text{F}$  coupling product **11** (CD $_2$ Cl $_2$ , 25 °C).

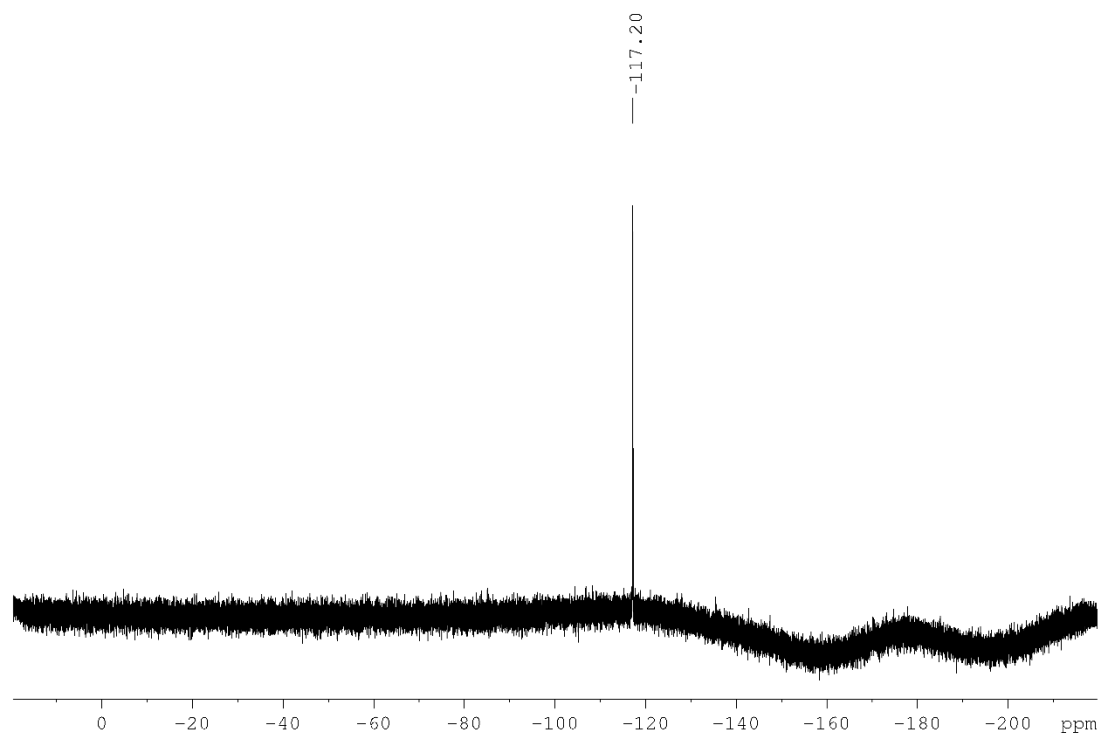


Figure 17,  $^{19}\text{F}$  NMR spectrum of the C-C $_6\text{H}_4\text{F}$  coupling product **11** (CD $_2$ Cl $_2$ , 25 °C).

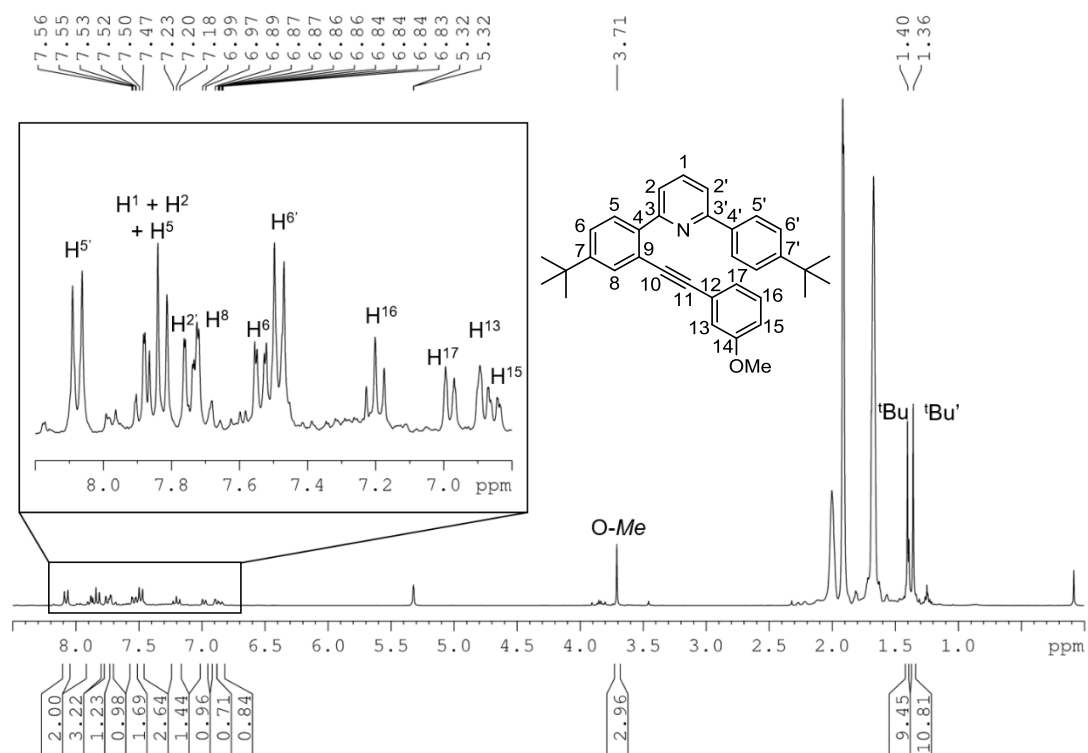


Figure 19, <sup>1</sup>H NMR spectrum of C-Acetylide coupling product **12** (CD<sub>2</sub>Cl<sub>2</sub>, 25 °C).

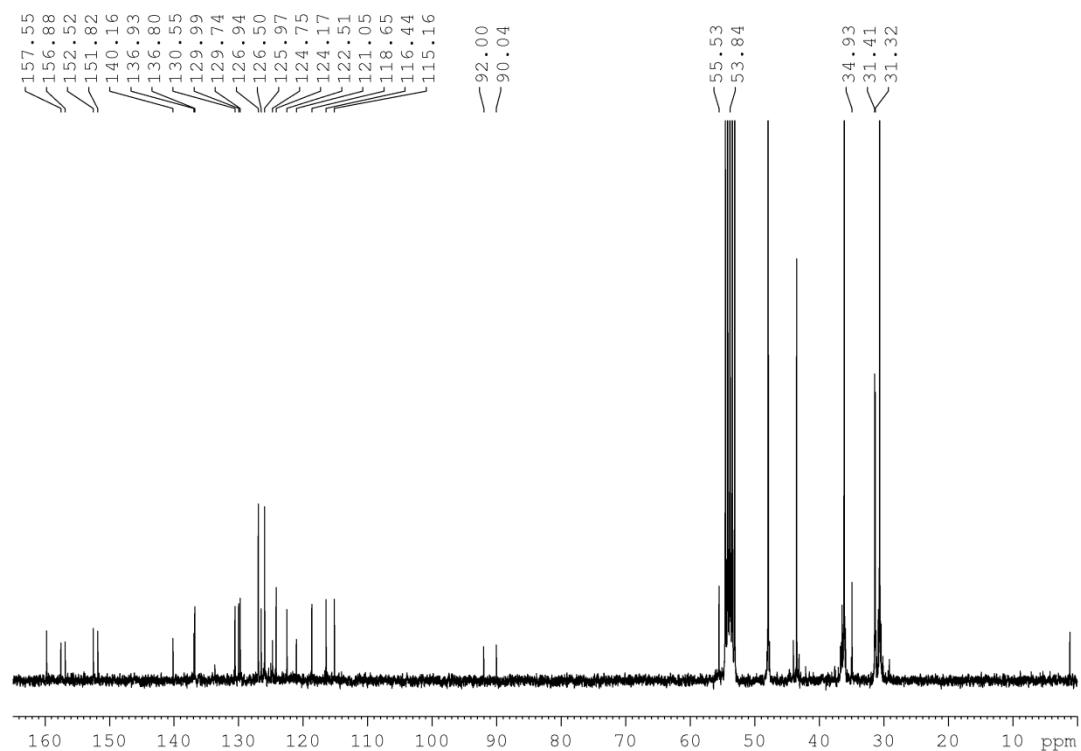


Figure 20, <sup>13</sup>C NMR spectrum of **12** (CD<sub>2</sub>Cl<sub>2</sub>, 25 °C).

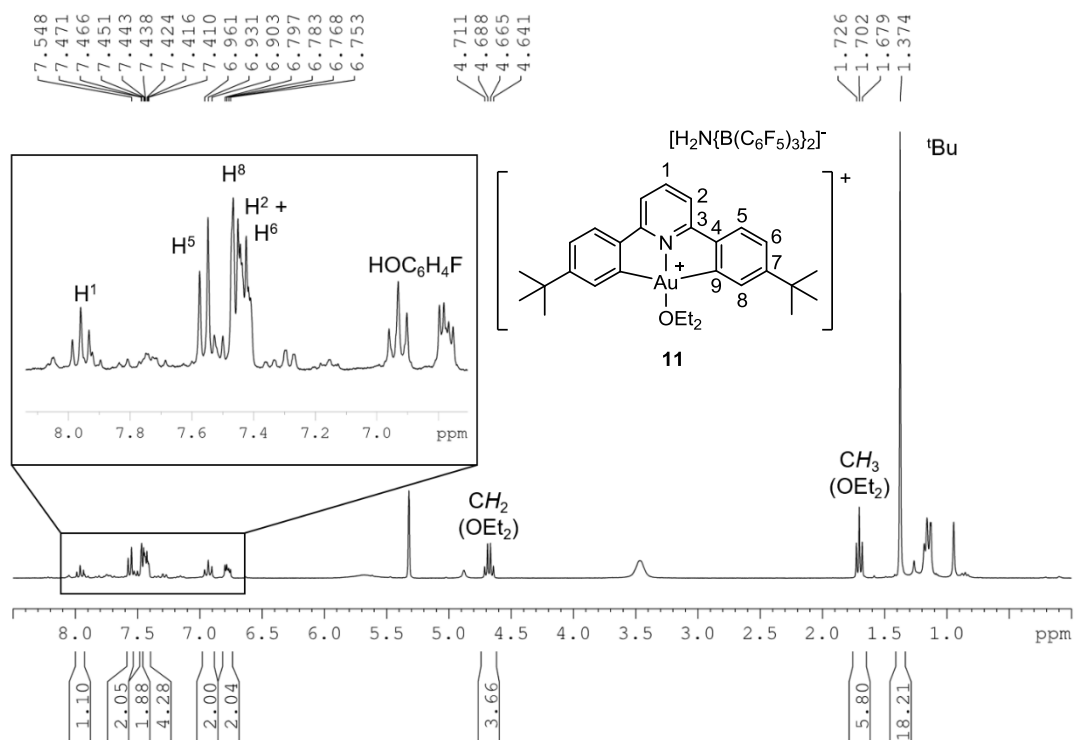


Figure 21, <sup>1</sup>H NMR spectrum of **14** (CD<sub>2</sub>Cl<sub>2</sub>, 25 °C).

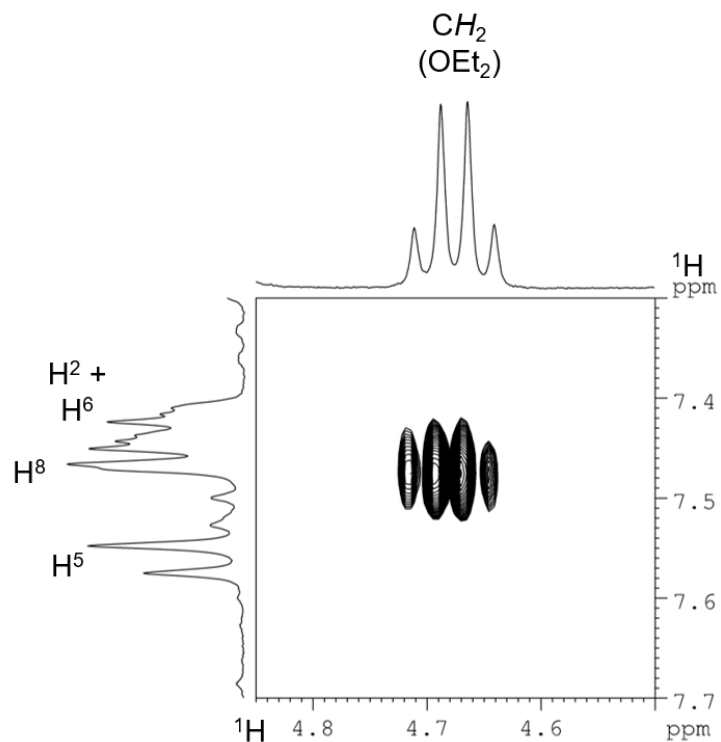


Figure 22, <sup>1</sup>H NOESY NMR spectrum of **14** (CD<sub>2</sub>Cl<sub>2</sub>, 25 °C).

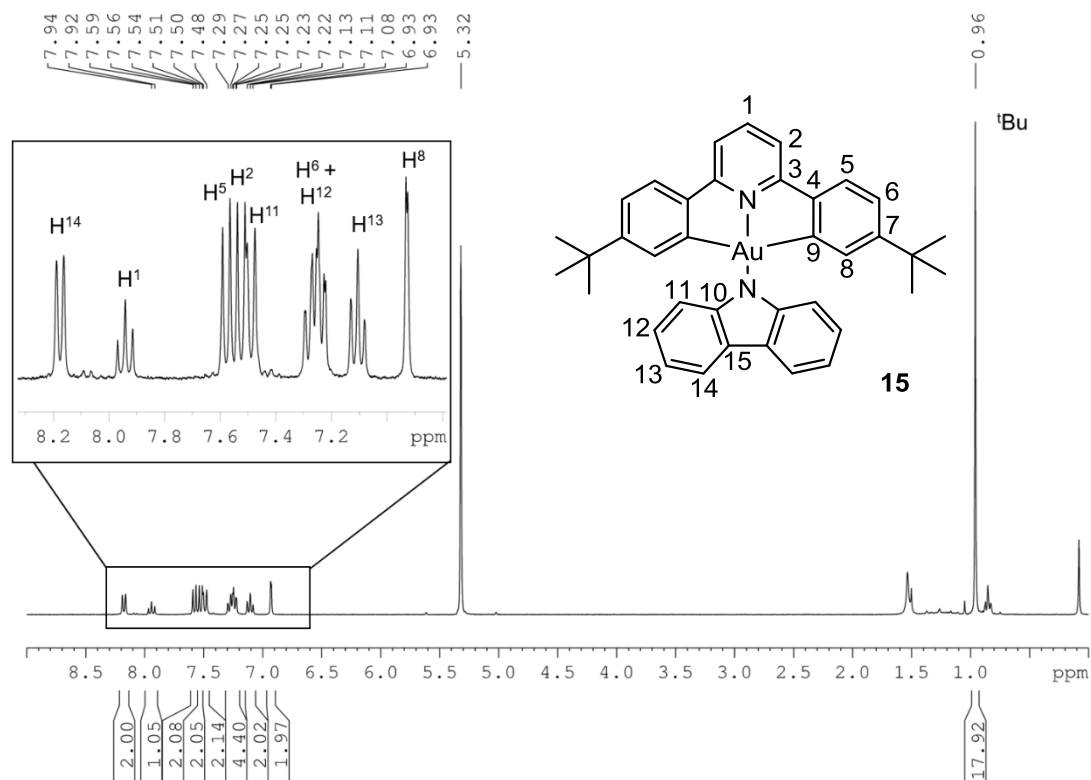


Figure 23, <sup>1</sup>H NMR spectrum of **15** (CD<sub>2</sub>Cl<sub>2</sub>, 25 °C).

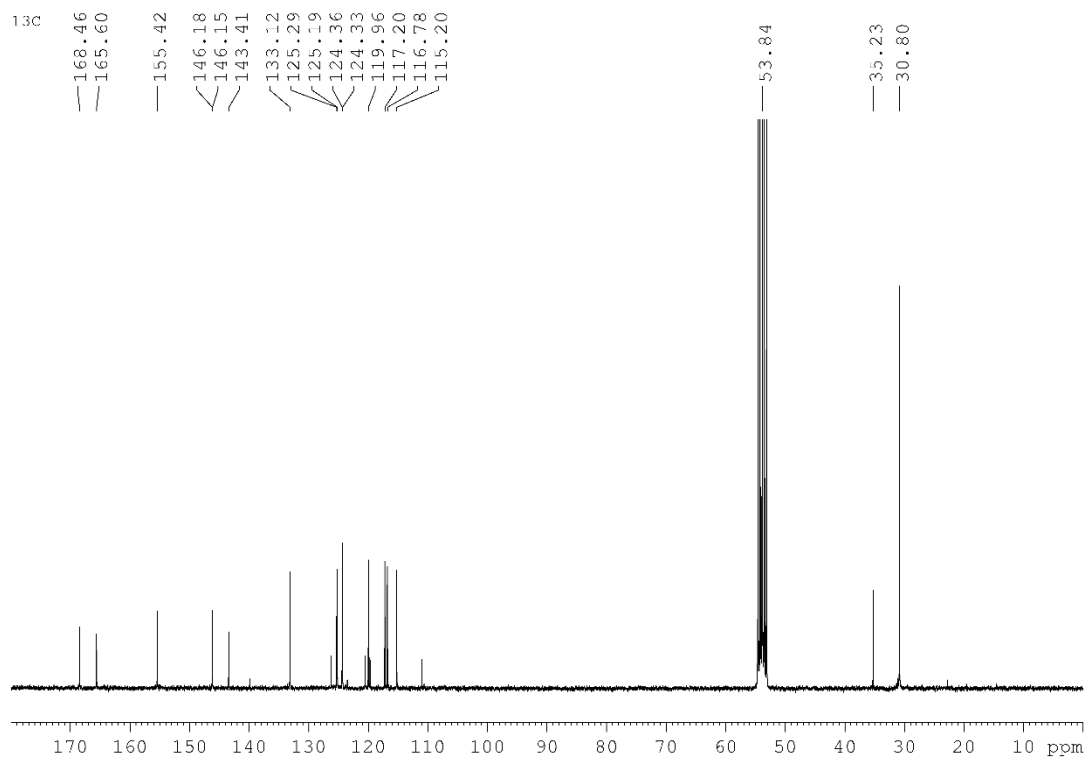


Figure 24, <sup>13</sup>C NMR spectrum **15** (CD<sub>2</sub>Cl<sub>2</sub>, 25 °C).

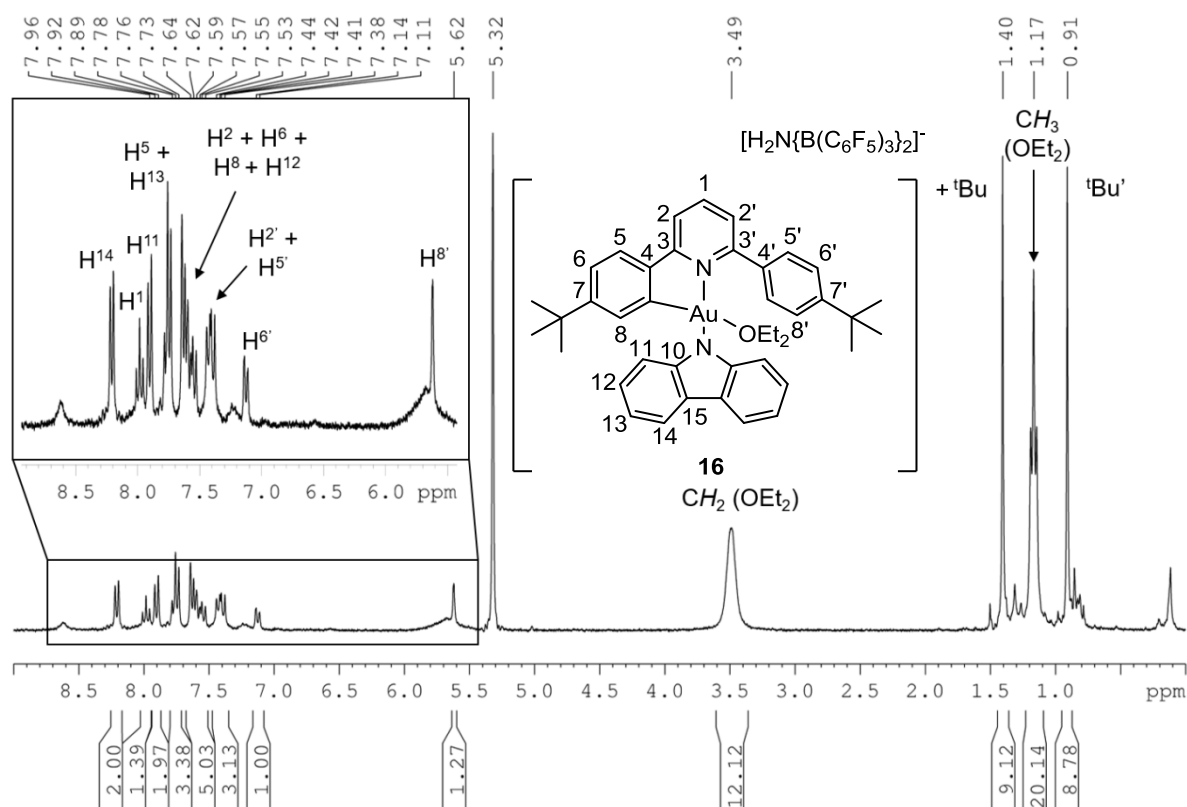


Figure 25,  $^1\text{H}$  NMR spectrum of **16** ( $\text{CD}_2\text{Cl}_2$ , 25  $^\circ\text{C}$ ).

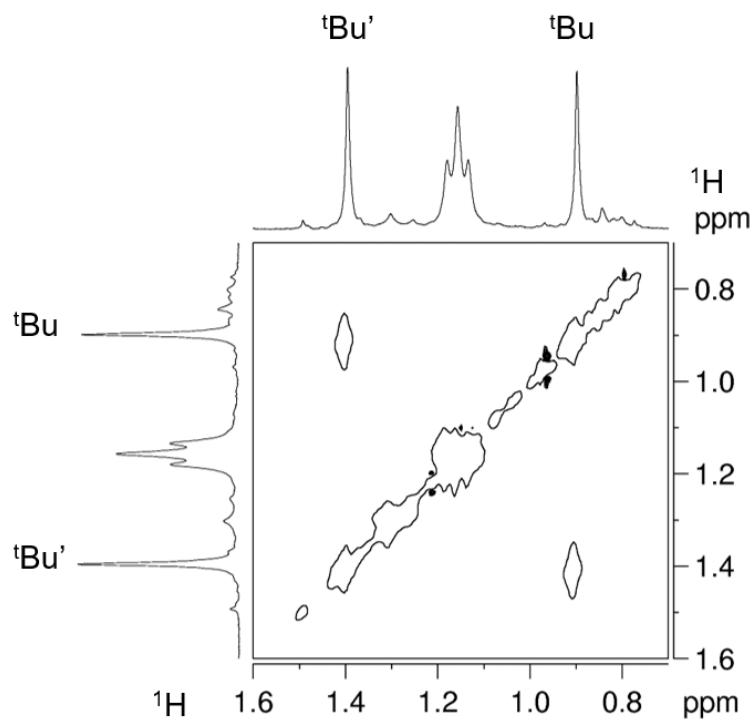


Figure 26, a section of the  $^1\text{H}$  NOESY NMR spectrum **16** showing chemical exchange between tertiary butyl signals ( $\text{CD}_2\text{Cl}_2$ , 25  $^\circ\text{C}$ ).